Conformation, Dynamics, and Structural Transitions of the TATA Box Region of Self-Complementary d[(C-G)$_n$-T-A-T-A-(C-G)$_n$] Duplexes in Solution

Dinshaw J. Patel*,‡ and Sharon A. Kozlowski

AT&T Bell Laboratories, Murray Hill, New Jersey 07974

Dennis R. Hare and Brian Reid

Chemistry Department, University of Washington, Seattle, Washington 98195

Satoshi Ikuta, Naphtali Lander, and Keiichi Itakura

Molecular Genetics Department, City of Hope National Medical Center, Duarte, California 91010

Received May 15, 1984

ABSTRACT: Structural and kinetic features of the TATA box located in the center of the alternating self-complementary d(C-G-C-G-T-A-T-A-C-G-C-G) duplex (TATA 12-mer) and d(C-G-C-G-C-G-T-A-T-A-C-G-C-G-C-G) duplex (TATA 16-mer) have been probed by high-resolution proton and phosphorus NMR spectroscopy in aqueous solution. The imino exchangeable Watson–Crick protons and the nonexchangeable base protons in the TATA box of the TATA 12-mer and TATA 16-mer duplexes have been assigned from intra and inter base pair nuclear Overhauser effect (NOE) measurements. Imino proton line-width and hydrogen exchange saturation recovery measurements demonstrate that the dA·dT base pairs in the TATA box located in the center of the TATA 12-mer and TATA 16-mer duplexes are kinetically more labile than flanking dG·dC base pairs. The proton and phosphorus NMR parameters of the TATA 12-mer monitor a cooperative premelting transition in the TATA box prior to the onset of the melting transition to unstacked strands. Phosphorus NMR studies have been unable to detect any indication of a right-handed B DNA to a left-handed Z DNA transition for the TATA 12-mer duplex in saturated NaCl solution. By contrast, we do detect the onset of the B to Z transition for the TATA 16-mer in saturated NaCl solution. Proton and phosphorus NMR studies demonstrate formation of a loop conformation with chain reversal at the TATA segment for the TATA 12-mer and TATA 16-mer duplexes on lowering the DNA and counterion concentration. The imino protons (10–11 ppm) and phosphorus resonances (3.5–4.0 ppm; 4.5–5.0 ppm) of the loop segment fall in spectral windows well resolved from the corresponding markers in fully paired segments so that it should be possible to identify loops in longer DNA helixes. The equilibrium between the loop and fully paired duplex conformations of the TATA 12-mer and TATA 16-mer is shifted toward the latter on addition of moderate salt.

Recent studies have demonstrated a sequence dependence to the conformation and dynamics of DNA fragments in the crystalline (Dickerson et al., 1982, 1983), solution (Patel et al., 1983a,b; Lu et al., 1983; Clore & Gronenborn, 1983), and fiber (Arnott et al., 1983) states. Specifically, the X-ray single-crystal structure of the d(C-G-C-G-A-A-T-T-C-G-C-G) duplex (AATT 12-mer) (Dickerson & Drew, 1981; Drew & Dickerson, 1981) and its detailed analysis (Calladine, 1982; Dickerson, 1983; Calladine & Drew, 1984) demonstrated that structural parameters such as base pair twist, slide, and roll were strongly dependent on sequence while base pair propeller twist and minor groove hydration differed between dA·dT and dG·dC base pairs. The AATT 12-mer duplex adopts a B-DNA conformation (Dickerson et al., 1982) in contrast to deoxyoctanucleotides (Shakked et al., 1981; Wang et al., 1982) that adopt the A conformation in the crystalline state. Sequence-dependent conformational variations are also detected in DNA fibers from studies of alternating (purine–pyrimidine)$_n$ on the one hand and homopolymers (purine)$_n$·(pyrimidine)$_n$ on the other (Arnott et al., 1983).

High-resolution proton NMR is a powerful method to probe the conformation of nucleic acids in solution (Redfield et al., 1981; Pardi et al., 1981; Patel et al., 1982a; Feigon et al., 1983; Haasnoot et al., 1983; Hare et al., 1983; Weiss et al., 1984). Thus, all the base and sugar protons in a sequence such as the AATT 12-mer can be partially and fully assigned by one-dimensional (Patel et al., 1982b) and two-dimensional (Hare et al. 1983) methods, respectively. Structural features such as propeller twist (Patel et al., 1983a), glycosidic torsion angles (Patel et al., 1982c; Clore & Gronenborn, 1983), and sugar pucker (Clore & Gronenborn, 1983) can be determined from an analysis of the distance-dependent nuclear Overhauser effects. The sequence dependence of the dynamics of DNA duplexes can be evaluated from hydrogen exchange measurements on the resolved and assigned Watson–Crick imino protons (Early et al., 1981a,b; Pardi & Tinoco, 1982). Thus, faster hydrogen exchange rates are demonstrated for the thymidine imino protons in the TATA box (Patel et al., 1983b) and the TGTG box (Lu et al., 1983) in DNA helixes. The hydrogen exchange rates are also very different in deoxynucleic acid, ribonucleic acid, and mixed nucleic acid duplexes at the oligomer (Pardi & Tinoco, 1982) and polymer (Mirau & Kearns, 1983) level.

There is considerable interest in the folding of unpaired segments in DNA, and much effort has been addressed toward the conformation and dynamics of hairpin and bulge loops in nucleic acids (Scheffler et al. 1968; Haasnoot et al., 1980;

‡Present address: Department of Biochemistry and Molecular Biophysics, Columbia University, New York, NY 10032.

0006-2960/85/0424-0926$01.50/0

Chart I

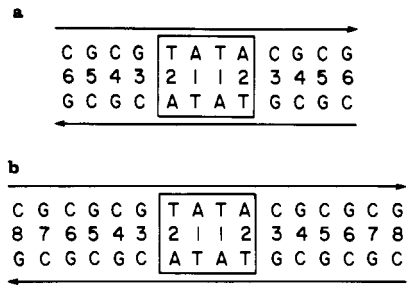

Marky & Olson, 1982). Thus, hairpin helix formation in the AATT 12-mer has been studied by optical, CD, and calorimetric measurements as a function of DNA concentration, ionic conditions, and temperature (Marky et al., 1983). Hairpin loop formation can be readily monitored by high-resolution NMR techniques (Haasnoot et al., 1983) and can provide useful information on the optimal size and flexibility of the loop, as well as accessibility of bases involved in chain reversal to solvent. The NMR research on hairpin loops has focused on sequences that cannot form perfect duplexes (Haasnoot et al., 1980, 1983), and there is a need to investigate the equilibrium between perfect duplexes and their loop conformations as a function of counterion and temperature.

The assignment of the salt-induced transition of $(dG\text{-}dC)_n$ (Pohl & Jovin, 1972) to an interconversion between right-handed B and left-handed Z forms (Wang et al., 1979) and its biological relevance (Klysik et al., 1981; Singleton et al., 1982; Nordheim & Rich, 1983; Rich et al., 1983, 1984; Jovin et al., 1983a; Haniford & Pulleyblank, 1983) have been the center of much attention. High-resolution proton and phosphorus NMR can readily monitor the dinucleotide repeat (Patel et al., 1979) and *syn*-glycosidic torsion angle (Patel et al., 1982c) in the Z-DNA helix. The potential of dA·dT base pairs imbedded in $(dC\text{-}dG)_n$ segments to undergo the B to Z transition is less well understood and needs clarification.

This paper reports on NMR studies of the d(C-G-C-G-T-A-T-A-C-G-C-G) duplex (TATA 12-mer, Chart Ia) and the d(C-G-C-G-C-G-T-A-T-A-C-G-C-G-C-G) duplex (TATA 16-mer, Chart Ib) in aqueous solution. We have assigned the exchangeable and nonexchangeable protons in the TATA box region by one-dimensional NOE measurements. The hydrogen exchange kinetics of the TATA box in both duplexes have been monitored from imino proton line-width and saturation recovery measurements. We demonstrate formation of loop conformations in the TATA 12-mer and TATA 16-mer at low DNA and counterion concentrations and at elevated temperature prior to the onset of the helix–coil transition. The potential of the TATA 12-mer and the TATA 16-mer to undergo the B to Z transition is investigated by phosphorus NMR spectroscopy. We have previously published on the assignment of the imino protons in the TATA 12-mer duplex and their hydrogen exchange characteristics by saturation recovery measurements (Patel et al., 1983b).

Experimental Procedures

NMR Spectroscopy. Proton NMR spectra of the imino exchangeable protons of the TATA 12-mer and TATA 16-mer were recorded in H_2O solution at 500 (Bruker instrument at the University of Washington, Seattle) and at 498 MHz (home-built spectrometer at the F. Bitter Magnet Laboratory, MIT) with a Redfield 214 pulse sequence to suppress the strong H_2O signal (Redfield et al., 1981). Nonexchangeable proton spectra were recorded on the 498-MHz Magnet Laboratory spectrometer and the Varian XL-200 spectrometer at AT&T Bell Laboratories. Proton chemical shifts are referenced relative to internal 5,5-dimethyl-5-silapentane-2-sulfonate (DSS). The nuclear Overhauser effect and saturation recovery data involving a set of decoupling frequencies or time delays were accumulated in the interleave mode. Phosphorus spectra were recorded with proton decoupling at 81 MHz on a Varian XL-200 spectrometer. The chemical shifts are referenced relative to internal trimethyl phosphate, are corrected for the temperature and salt dependence of the standard, and are calibrated relative to no added salt at 27 °C.

Synthesis. The TATA 12-mer and TATA 16-mer sequences were synthesized in milligram amounts by the solid-phase triester method reported previously (Tan et al., 1983). The procedure consists of attaching the 3′-terminal nucleoside of the desired sequence to the polystyrene copolymer support through 1% divinylbenzene linkage. The mononucleotide or dinucleotide coupling units were sequentially added through their 3′-ends to the growing nucleotide chain on the insoluble support until the desired sequence was built. The dimer coupling yields ranged from 88 to 92%. The final product was cleaved from the solid support, the protecting groups were deblocked, and the oligonucleotide was purified on DEAE-cellulose DE-52 followed by size-exclusion chromatography on Sephadex G-75 or G-50. The high-temperature proton NMR spectra of the TATA 12-mer and the TATA 16-mer confirmed the purity of the oligonucleotides.

Concentration. The proton and phosphorus NMR investigation of the TATA 12-mer and TATA 16-mer was undertaken at high DNA (100 A_{260} units in 0.3 mL) and low DNA (10 A_{260} units in 0.3 mL) concentrations. We could record one-dimensional NOEs readily at a concentration of 100 A_{260}/0.3 mL but could not undertake two-dimensional experiments because of signal to noise limitations. The concentrations are presented in A_{260} units per milliliter in the remainder of the text.

Results

Resonance Assignments. The NMR markers are distributed among the exchangeable protons, the nonexchangeable protons, and the backbone phosphates of DNA. We have assigned several of these markers in the TATA 12-mer and TATA 16-mer (333 A_{260}/mL) in 0.1 M phosphate by one-dimensional NOE experiments, and the results are summarized below.

(*A*) *Imino Protons.* Previous studies have demonstrated that the thymidine and guanosine imino protons of dA·dT and dG·dC base pairs of nucleic acids resonate between 12.5 and 14.5 ppm in H_2O solution. The imino protons from the five nonterminal base pairs are well resolved in the TATA 12-mer (Patel et al., 1983b) while there is only partial resolution of the seven nonterminal base pairs in the TATA 16-mer in 0.1 M phosphate at low temperature (Figure 1A).

The imino protons in the TATA 12-mer were assigned previously (Patel et al., 1983b), and the approach is extended to assignment of the internal imino protons in the TATA 16-mer duplex. The imino proton of the TATA 16-mer in 0.1 M phosphate–H_2O, pH 6.67 at 5 °C between 6 and 14 ppm is presented in Figure 1A. We observe resolved resonances in the imino (12–14 ppm) and the aromatic (7–9 ppm) spectral regions. The imino protons in the interior of the TATA 16-mer duplex have been assigned from one-dimensional NOE experiments (saturation time 1 s), which monitor both intra and inter base pair interactions. Thus, saturation of the 13.247 ppm imino proton results in an intra base pair NOE to a narrow resonance at 7.125 ppm (Figure 1C), and this is

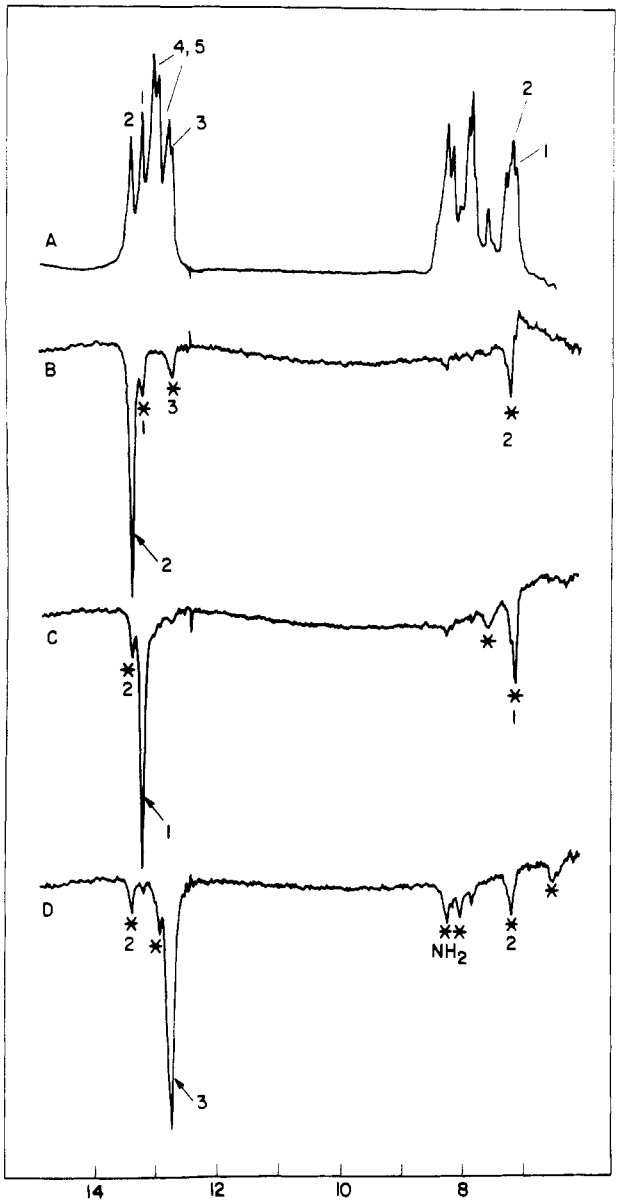

FIGURE 1: (A) The 498-MHz proton Fourier-transform spectrum (6–14 ppm) of the TATA 16-mer duplex (333 A_{260}/mL) in 0.1 M phosphate, 2.5 mM EDTA, and 4:1 H_2O/D_2O, pH 6.67 at 5 °C. The imino proton assignment to specific base pairs are designated over the resonances. Difference spectra following 1-s saturation of (B) the 13.432 ppm thymidine imino proton, (C) the 13.247 ppm thymidine imino proton, and (D) the 12.761 ppm guanosine imino proton in the TATA 16-mer duplex. The saturated resonance is designated by an arrow while the intra base pair NOEs in the aromatic region (6.0–8.5 ppm) and the inter base pair NOEs in the imino region (12.5–14.0 ppm) are designated by asterisks. The signal to noise in the spectra was improved by applying a 5-Hz line-broadening contribution.

characteristic of a thymidine imino to adenosine H-2 NOE in a dA·dT base pair. Further, a single inter base pair NOE is observed at the 13.432 ppm imino proton (Figure 1C), which requires that the 13.247 and 13.432 ppm imino protons be assigned to dA·dT base pairs 1 and 2, respectively, in the TATA 16-mer duplex (Chart Ib).

Saturation of the 13.432 ppm imino proton of dA·dT base pair 2 results in an intra base pair NOE to the adenosine H-2 at 7.197 ppm and inter base pair NOEs to the iminos of adjacent dA·dT base pair 1 at 13.243 ppm and dG·dC base pair 3 at 12.761 ppm (Figure 1B). Saturation of the 12.761 ppm imino proton of dG·dC base pair 3 results in intra base pair NOEs at the 8.257 and 8.042 ppm amino protons and to the 13.424 ppm imino and 7.193 ppm adenosine H-2 protons

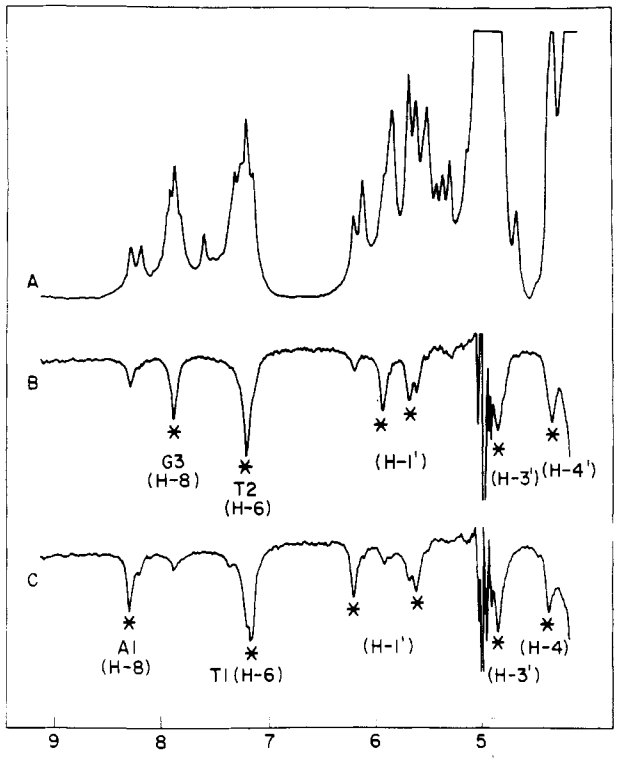

FIGURE 2: (A) The 498-MHz proton NMR spectrum (4–9 ppm) of the TATA 16-mer duplex (333 A_{260}/mL) in 0.1 M phosphate, 2.5 mM EDTA, and D_2O, pH 7.03 at 5 °C. The difference spectra following 1-s saturation of (B) the thymidine CH_3-5 resonance at 1.478 ppm and (C) the thymidine CH_3-5 resonance at 1.390 ppm. The observed NOEs in the difference spectra are designated by asterisks.

of adjacent dA·dT base pair 2 in the TATA 16-mer duplex (Figure 1D). There is insufficient resolution to unambiguously assign the remaining dG·dC imino protons by one-dimensional NOE experiments.

(*B*) *Nonexchangeable Base Protons.* The nonexchangeable purine and pyrimidine base and sugar H-1′ protons resonate between 5.0 and 8.5 ppm in the spectra of the TATA 12-mer and the TATA 16-mer (Figure 2A) duplexes at low temperature. The base protons line both the minor and major grooves and, hence, provide usful markers for monitoring ligand–DNA interactions. Resonance assignments can be made from NOE measurements, and we focus our efforts on assigning the base protons from dA·dT pairs 1 and 2 in the center of the TATA 16-mer duplex at 5 °C (Figure 2A).

We can differentiate between dA·dT base pairs 1 and 2 on the basis of a detectable NOE between the purine H-8 and pyrimidine CH_3-5 in the pyrimidine(3′–5′)purine step in right-handed DNA. Thus, 1-s saturation of the CH_3-5 at 1.478 ppm results in an NOE at the 7.223 ppm proton of its own thymidine H-6 and the 7.990 ppm proton of an adjacent guanosine H-8 resonance (Figure 2B). This inter base pair NOE must correspond to the $G_3(3'\text{-}5')T_2$ step in the TATA 16-mer duplex (Chart Ib), permitting assignment of the 7.223 ppm H-6 and the 1.478 ppm CH_3-5 to the thymidine at position 2 in the sequence.

By contrast, saturation of the 1.390 ppm thymidine CH_3-5 results in an NOE at the 7.181 ppm thymidine H-6 of the same base and the 8.305 ppm adenosine H-8 of the flanking base (Figure 2C). This inter base pair NOE must correspond to the $A_1(3'\text{-}5')T_1$ step in the TATA 16-mer (Chart Ib), permitting assignment of the 7.181 ppm H-6 and the 1.390 ppm CH_3-5 to the thymidine at position 1 in the TATA 16-mer duplex at 5 °C. Since the 8.305 ppm adenosine H-8 is assigned to position 1, the remaining adenosine H-8 at 8.213 ppm is

Table I: Exchangeable and Nonexchangeable Base Proton Chemical Shifts of dA·dT Base Pairs 1 and 2 in the TATA 12-mer and TATA 16-mer Duplexes in 0.1 M Phosphate at 5 °C

	chemical shift (ppm)			
	TATA 12-mer		TATA 16-mer	
resonance	1	2	1	2
T H-3	13.287	13.440	13.247	13.432
T H-6	7.189	7.235	7.181	7.223
T CH_3-5	1.408	1.508	1.390	1.478
A H-8	8.317	8.231	8.305	8.213
A H-2	7.185	7.267	7.125	7.197

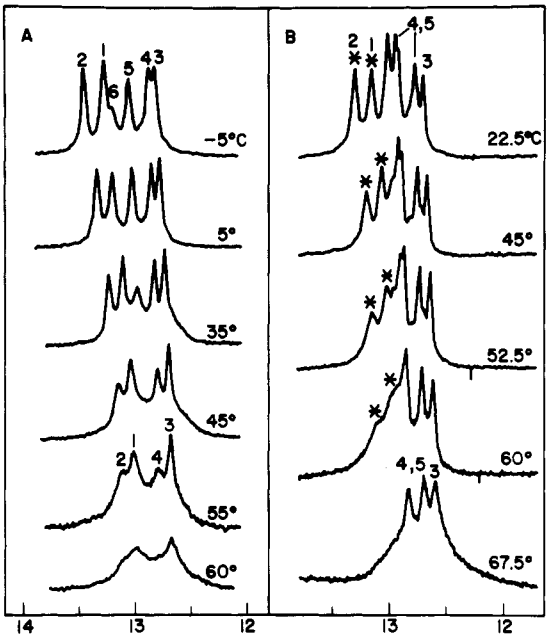

FIGURE 3: Temperature-dependence 498-MHz proton NMR spectra of (A) the TATA 12-mer at pH 7.20 and (B) the TATA 16-mer at pH 6.67 in 0.1 M phosphate–H_2O solution. The DNA concentration was 333 A_{260}/mL. The imino proton assignments to specific base pairs are designated over the resonances.

assigned to position 2 in the sequence. The base proton chemical shifts at positions 1 and 2 in the center of the TATA 12-mer and TATA 16-mer duplexes in 0.1 M phosphate at 5 °C are listed in Table I.

Hydrogen Exchange. The exchangeable imino protons are useful markers for monitoring hydrogen exchange in nucleic acids (Redfield et al., 1981). The exchange kinetics can be probed by monitoring the imino proton line widths (Patel & Hilbers, 1975; Fritzche et al., 1983) or alternately from saturation recovery measurements (Early et al., 1981a,b; Pardi & Tinoco, 1982). These experiments have been undertaken on the TATA 12-mer and TATA 16-mer (333 A_{260}/mL) in 0.1 M phosphate and are described below.

(A) Line-Width Measurements. We have recorded the imino proton spectra of the TATA 12-mer (pH 7.20) and the TATA 16-mer (pH 6.67) in 0.1 M phosphate as a function of temperature, and these are compared in panels A and B of Figure 3, respectively. We note that fraying at the ends of the TATA 12-mer helix results in broadening of the imino proton of base pair 6 by 5 °C and base pair 5 by 45 °C (Figure 3A). It is further apparent that the imino protons of dA·dT base pairs 1 and 2 in the center of the TATA 12-mer duplex broaden at a somewhat lower temperature than that of flanking dG·dC base pair 3 at 60 °C (Figure 3A).

This atypical broadening behavior in the center of the duplex is observed even more clearly for the imino protons of the TATA 16-mer in 0.1 M phosphate between 22.5 and 67.5 °C

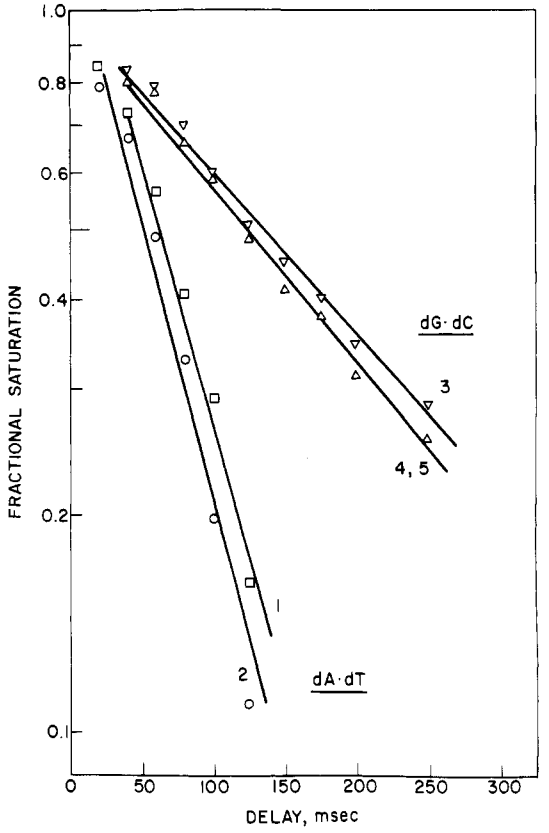

FIGURE 4: Semilogarithmic plots of the fractional saturation of dA·dT base pairs 1 (□) and 2 (○) and dG·dC base pairs 3 (▽) and 4/5 (△) in the TATA 16-mer as a function of the delay between the saturation and observation pulses in millisecond at 37.5 °C. The buffer was 0.1 M phosphate, 2.5 mM EDTA, and 4:1 H_2O/D_2O, pH 6.67. The DNA concentration was 333 A_{260}/mL.

Table II: Saturation Recovery Lifetimes (ms) of the Imino Protons of the TATA 12-mer and TATA 16-mer and Comparison with AATT 12-mer Data in 0.1 M Phosphate at 37.5 °C

	dG·dC		dA·dT	
	4	3	2	1
TATA 12-mer[a]	177	228	51	70
TATA 16-mer[b]	180	194	56	59
AATT 12-mer[c]	170	283	114	172

[a] pH 6.54. [b] pH 6.67. [c] pH 6.95.

(Figure 3B). We note that the imino protons of dA·dT base pairs 1 and 2 broaden prior to the imino protons of flanking dG·dC base pairs 3–5 in the 67.5 °C spectrum of the TATA 16-mer duplex (Figure 3B). The imino proton line-width data in the TATA 12-mer and the TATA 16-mer demonstrate fast hydrogen exchange rates in the TATA box segment in the center of the duplex.

(B) Saturation Recovery Measurements. We have monitored the hydrogen exchange kinetics of the imino protons of dA·dT base pairs 1 and 2 and flanking dG·dC base pairs in the TATA 16-mer duplex in 0.1 M phosphate, pH 6.7, from saturation recovery measurements. The recovery of magnetization at these imino protons as a function of the delay between the saturation and observation pulses is plotted for the TATA 16-mer at 34.5 °C in Figure 4. The imino protons of the central dA·dT base pairs 1 and 2 exhibit recovery lifetimes between 55 and 60 ms while those of flanking dG·dC base pairs 3 and 4 exhibit lifetimes between 180 and 195 ms (Figure 4, Table II). The hydrogen exchange contribution to the saturation recovery data predominates above room temperature as demonstrated from our detailed temperature-

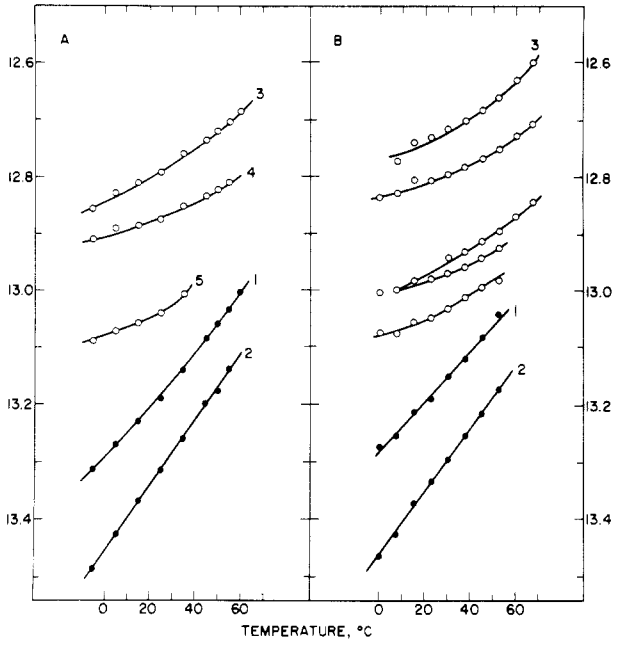

FIGURE 5: Temperature dependence of the imino proton chemical shifts of (A) the TATA 12-mer at pH 7.20 and (B) the TATA 16-mer at pH 6.57 in 0.1 M phosphate–H_2O solution. The DNA concentration was 333 A_{260}/mL. The imino proton assignments to specific base pairs are designated in the plots.

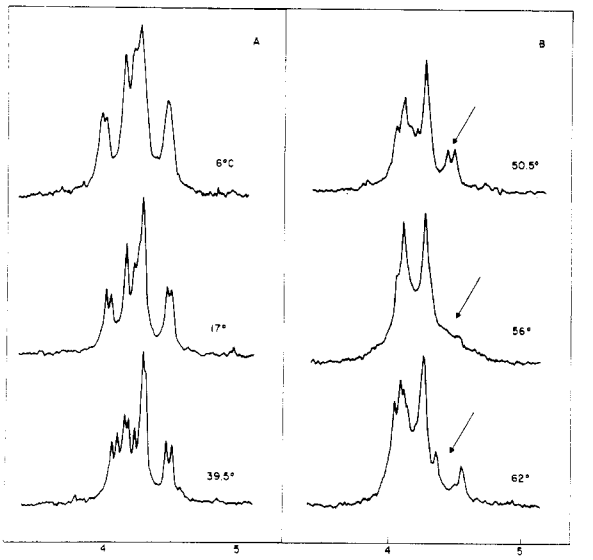

FIGURE 6: Proton noise-decoupled 81-MHz phosphorus spectra of the TATA 12-mer in 50 mM phosphate–D_2O, pH 7.34 at (A) 6, 17, and 39.5 °C and (B) 50.5, 56, and 62 °C. The DNA concentration was 167 A_{260}/mL. The chemical shifts have been corrected for the temperature dependence of the internal trimethyl phosphate standard and are relative to the value at 27 °C.

and pH-dependent studies of saturation recovery kinetics of the TATA 12-mer (Patel et al., 1983b).

(C) Sequence Dependence. The saturation recovery lifetimes of dA·dT base pairs 1 and 2 and dG·dC base pairs 3 and 4 in the TATA 12-mer, TATA 16-mer, and AATT 12-mer duplexes in 0.1 M phosphate, 37.5 °C, are compared in Table II. The lifetimes for these four internal positions are comparable in the TATA 12-mer and TATA 16-mer duplexes (Table II). However, the exchange rates, which are a measure of the transient duplex opening rates, are a factor of 2–3 faster for the imino protons of the TATA box in the TATA 12-mer and TATA 16-mer duplexes compared to those of the AATT segment in the AATT 12-mer duplex (Table II).

Premelting Transition. The premelting conformational transitions observed for DNA duplexes can be readily monitored by the chemical shift changes for the exchangeable and nonexchangeable nucleic acid base and sugar protons in the temperature range below the duplex to strand transition. This is especially evident in the TATA 12-mer and TATA 16-mer spectra (333 A_{260}/mL) in 0.1 M phosphate, and the results are presented below.

(A) Noncooperative Transition. The temperature dependence of the imino proton chemical shifts of the TATA 12-mer and the TATA 16-mer in 0.1 M phosphate are plotted in panels A and B of Figure 5, respectively. The largest temperature dependence is observed for the imino protons of dA·dT base pairs 1 and 2 in the center of the duplex while the imino protons of the flanking dG·dC base pairs exhibit similar moderate temperature-dependent shifts (Figure 5). We also observe noncooperative chemical shift changes for the nonexchangeable base protons of dA·dT base pairs 1 and 2 in the TATA 12-mer and TATA 16-mer duplexes.

(B) Cooperative Transition. We have monitored a cooperative transition between the fully paired TATA 12-mer duplex and another conformation between 50 and 60 °C prior to the onset of the melting transition at higher temperature. The 11 phosphodiesters are partially resolved in the proton-decoupled 81-MHz phosphorus spectrum of the TATA 12-mer (167 A_{260}/mL) in 50 mM phosphate at room temperature (Figure 6A). A simple procedure for phosphorus assignments in nucleic acids has been recently proposed on the basis of selective ^{17}O labeling and resultant broadening of individual phosphates in DNA (Petersheim et al., 1984; Joseph & Bolton, 1984; Connolly & Eckstein, 1984). It was demonstrated that the phosphorus resonances shift to high field on proceeding from the ends to the interior of the duplex (Connolly & Eckstein, 1984). We tentatively assign the phosphates at 4.46 and 4.50 ppm in the TATA 12-mer spectrum (Figure 6A) to the phosphodiesters in the TATA central portion of the dodecanucleotide.

The temperature dependence of the 11 partially resolved phosphodiesters of that TATA 12-mer in 50 mM phosphate between 7 and 62 °C is shown in Figure 6. There are small variations in the spectral pattern between 6 and 50.5 °C in the temperature range where the proton resonances monitor a noncooperative premelting transition (Figure 6A). By contrast, dramatic changes are detected at the upfield pair of phosphorus resonances assigned to the central TATA box of the TATA 12-mer between 50.5 and 62 °C. Thus, the 4.45 and 4.50 ppm resonances at 50.5 °C broaden in the 56 °C spectrum and are then replaced by resonances at 4.37 and 4.56 ppm in the 62 °C spectrum (Figure 6B). These changes monitor a cooperative conformational transition in the TATA segment of the dodecanucleotide duplex prior to the onset of the melting transition.

Similar changes are detected in the nonexchangeable base protons of dA·dT base pairs 1 and 2 of the TATA 12-mer in 0.1 M phosphate between 50 and 65 °C. Thus, the 1.42 and 1.50 ppm thymidine CH_3-5 protons at positions 1 and 2 in the TATA 12-mer undergo downfield shifts between 50 and 65 °C, indicative of a less stacked environment for these thymidines during this cooperative premelting transition. Further, downfield shifts are detected as this TATA 12-mer conformation undergoes a cooperative melting transition to unstacked strands at ~73 °C.

Z-Helix Formation. The B to Z transition for $(dC\text{-}dG)_n$ duplexes (Pohl & Jovin, 1972; Wang et al., 1979) can be readily monitored by phosphorus NMR spectroscopy (Patel

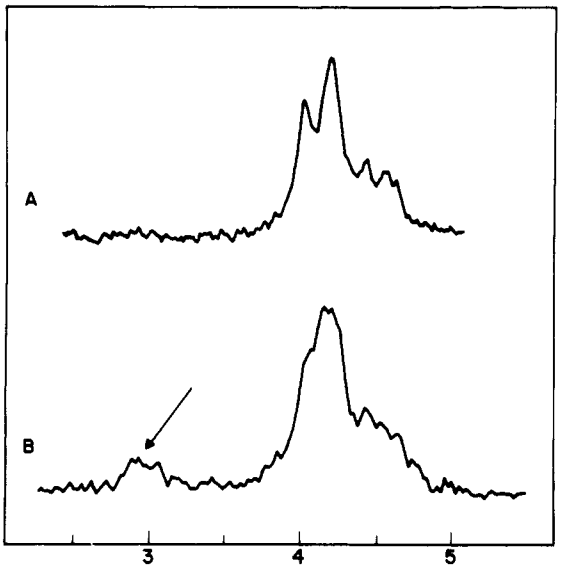

FIGURE 7: Proton noise-decoupled 81-MHz NMR spectrum of the (A) the TATA 12-mer and (B) the TATA 16-mer in saturating NaCl in 50 mM phosphate, 1.25 mM EDTA, and D_2O at 35.5 °C. The DNA concentration was 167 A_{260}/mL. The signal to noise of the spectra was improved by applying a 1-Hz line-broadening contribution. The chemical shifts have been corrected for the salt and temperature dependence of the internal standard trimethyl phosphate and are relative to the value of no added salt at 27 °C.

et al., 1979). Thus, the GpC and CpG phosphates exhibit similar chemical shifts at ~4.2 ppm in the mononucleotide-repeat right-handed B DNA in low salt but give two well-resolved resonances of equal arrea at ~3.0 and ~4.2 ppm in the dinucleotide-repeat left-handed Z DNA (Patel et al., 1979, 1982). Thiophosphate labeling studies have permitted assignment of the ~3.0 ppm resonance to GpC and the ~4.2 ppm resonance to CpG in the Z-DNA helix (Eckstein, 1983; Jovin et al., 1983b). We have used these phosphorus markers to monitor potential Z-DNA formation in the TATA 12-mer and TATA 16-mer helixes (167 A_{260}/mL) in saturated salt solution.

We do not detect any resonances at ~3 ppm in the TATA 12-mer phosphorus spectrum in 5 M NaCl–50 mM phosphate at 35.5 °C (Figure 7A), demonstrating that the dodecanucleotide does not switch to Z DNA in high-salt solution.

We detect a minor resonance at ~3 ppm in the phosphorus spectrum of the TATA 16-mer in saturating NaCl solution–50 mM phosphate at 35.5 °C (Figure 7B). Its relative area compared to the envelope between 4.0 and 4.8 ppm demonstrates that ~11% of the TATA 16-mer has switched to Z DNA in high-salt solution. Thus, incorporation of a TATA block into the center of an otherwise $(dC\text{-}dG)_n$ duplex results in an inhibition of the B to Z transition.

Loop Conformation. The proton NMR spectra on the TATA 12-mer duplex reported in the previous sections were recorded at high DNA concentrations (333 A_{260}/mL) in 100 mM phosphate solution (Figures 1–5). These samples were diluted by a factor of 2 to record the phosphorus spectra (Figures 6 and 7). Proton and phosphorus NMR spectra detected a new conformation of the TATA 12-mer on lowering the DNA concentration by a factor of 10 (33 A_{260}/mL) at low counterion concentrations (1 mM phosphate).

(A) Imino Protons. The proton spectra (6–14 ppm) of the TATA 12-mer in H_2O solution at low DNA (33 A_{260}/mL) and low counterion (1 mM phosphate) concentrations in the presence and absence of 0.4M NaCl at 0 °C are presented in panels A and B of Figure 8, respectively. The imino proton

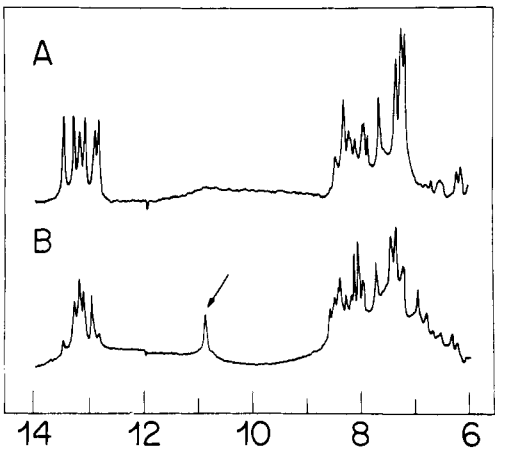

FIGURE 8: The 500-MHz proton spectra of the hydrogen-bonded imino (12.5–14 ppm), nonpaired imino (10–11 ppm), and base (6.5–9 ppm) protons of the TATA 12-mer (33 A_{260}/mL) in (A) the presence of 0.4 M NaCl and with (B) no added NaCl in 1 mM phosphate at 0 °C.

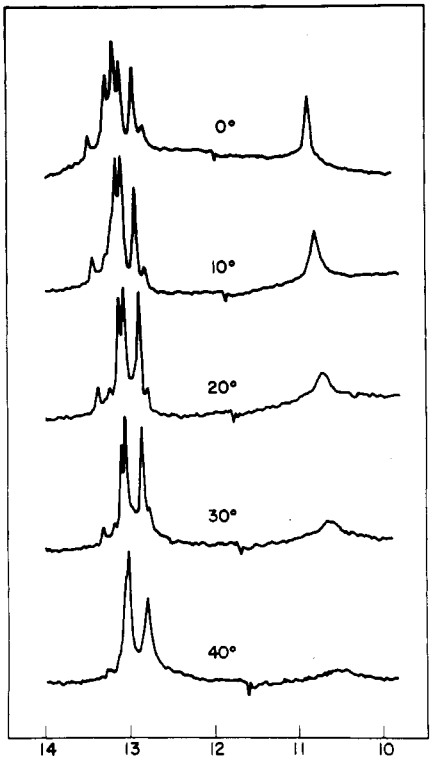

FIGURE 9: The 500-MHz proton spectra of the hydrogen-bonded imino (12.5–14 ppm) and nonpaired imino (10–11 ppm) of the TATA 12-mer (33 A_{260}/mL) in the absence of added salt in 1 mM phosphate–H_2O between 0 and 40 °C.

spectral region in the presence of 0.4 M NaCl exhibits six resolved resonances between 12.8 and 13.5 ppm at 0 °C (Figure 8A) corresponding to the six unique base pairs in the fully paired self-complementary duplex (Chart Ia).

By contrast, the predominant conformation of the TATA 12-mer in the absence of added NaCl at 0 °C exhibits four resolvable imino resonances between 12.9 and 13.2 ppm and a resonance(s) at 10.95 ppm (Figure 8B). These results suggest formation of a loop conformation stabilized by four dG·dC base pairs with the TATA segment involved in chain reversal. The observation of resonance(s) at 10.95 ppm is indicative of slow exchange of imino protons of thymidine bases in the loop with solvent H_2O and suggests that this (these) imino proton(s) is (are) partially shielded from solvent

(Haasnoot et al., 1980, 1983). The temperature dependence of the imino protons of the TATA 12-mer in the absence of added salt between 0 and 40 °C is presented in Figure 9. Specifically, one of the imino protons in the base-paired region centered about 13 ppm completely disappears while the imino proton(s) in the loop region centered about 11 ppm broadens significantly on raising the temperature. The resonance at low field that broadens out is most likely the terminal dG·dC base pair 6, which broadens out due to fraying at the ends of the helix (Patel & Hilbers, 1975). The results indicate that the imino protons in the loop exhibit an exchange rate intermediate between terminal and internal imino protons in base-paired stem regions. The above studies demonstrate that at a fixed low concentration of DNA and counterion it is possible to reversibly switch the TATA 12-mer between loop and fully paired helixes as a function of moderate salt concentrations.

(*B*) *Nonexchangeable Protons.* The aromatic base and amino protons resonate between 7 and 8.5 ppm in the TATA 12-mer spectra of the fully paired duplex (Figure 8A) and the loop conformation (Figure 8B). The adenosine H-2 protons can be readily identified in this spectral dispersion since they exhibit the longest spin–lattice relaxation times due to their isolation from other nonexchangeable protons in D_2O solution. The spin–lattice relaxation time measurements demonstrate that the H-2 protons of adenosine residues 1 and 2 in the TATA 12-mer resonated between 7.2 and 7.3 ppm in the fully paired duplex (Figure 8A) and between 8.0 and 8.1 ppm in the loop conformation (Figure 8B). The adenosine H-2 protons resonate to high field (7.2–7.3 ppm) in the duplex state since they experience upfield ring current contributions from adjacent base-pair purines on the partner strand (Giessner-Prettre et al., 1976). By contrast, in the loop conformation the observed adenosine H-2 shifts (8.0–8.1 ppm) are characteristic of strand states and reflect the loss of purine ring current contributions due to the absence of a partner strand. These results are consistent with chain reversal at the TATA segment of the TATA 12-mer loop conformation.

(*C*) *Backbone Phosphates.* Previous studies have demonstrated a dispersion of phosphorus resonances between 4.0 and 4.5 ppm in the proton-decoupled phosphorus spectra of fully paired duplexes (Patel, 1976; Gorenstein et al., 1976). By contrast, resolved phosphorus resonance to low and high field of the 4.0–4.5 ppm spectral dispersion has been observed in transfer RNA (Gueron & Shulman, 1975), and some of these shifted phosphodiesters have been assigned to hairpin loops in the secondary structure (Salemink et al., 1981) and also to bond angle distortions in the tertiary structure (Gorenstein & Luxon, 1979).

The proton noise decoupled phosphorus spectra of the TATA 12-mer (Figure 10A) and the TATA 16-mer (Figure 10B) at low DNA concentration (33 A_{260}/mL) and low counterion concentration (1 mM phosphate) exhibit phosphorus spectra to low field (~3.7 ppm) and to high field (~4.6 and ~5.0 ppm) of the central cluster dispersed between 4.0 and 4.5 ppm. The shifted phosphodiesters suggest formation of a loop conformation in which a portion of the phosphate backbone adopts a structure other than a fully paired duplex.

We have monitored the temperature dependence of the resolved phosphodiesters in the loop conformation of the TATA 12-mer at low DNA and counterion concentration to determine the constraints on the loop conformation in the temperature range prior to unstacked strand formation. The resolved phosphorus resonances at 4.6 and 5.0 ppm exhibit temperature-independent shifts between 0 and 30 °C and then gradually move downfield into the 4.0–4.5 ppm region on raising the temperature to 65 °C (Figure 10C). This suggests that the constraints on the conformation of the loop are relaxed between 40 and 65 °C prior to the onset of the melting transition above this temperature.

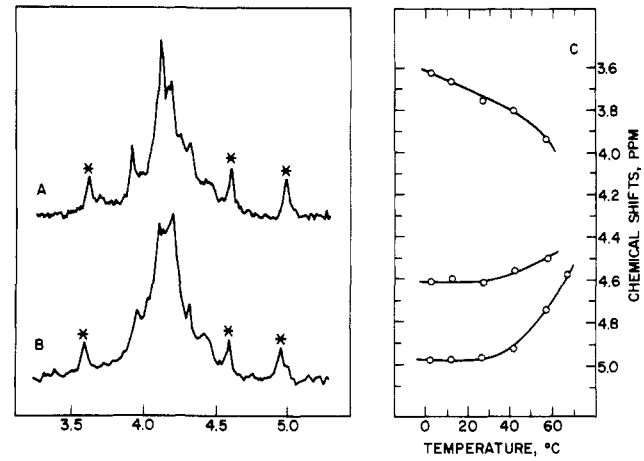

FIGURE 10: Proton noise-decoupled 81-MHz phosphorus NMR spectra of (A) the TATA 12-mer (33 A_{260}/mL) at 2 °C and (B) the TATA 16-mer (33 A_{260}/mL) at 7 °C in low phosphate buffer. Chemical shifts are referenced relative to internal trimethyl phosphate. (C) The temperature dependence of the resolved (see asterisks) phosphates in the TATA 12-mer (33 A_{260}/mL) in 1 mM phosphate between 0 and 60 °C.

Discussion

This paper focuses on the structural and dynamic features of the TATA box located in the center of the TATA 12-mer (Chart Ia) and TATA 16-mer (Chart Ib) duplexes.

Assignments. The exchangeable and nonexchangeable protons in the TATA box of the two duplexes can be readily assigned from one-dimensional NOE experiments (Figures 1 and 2), and the chemical shifts are summarized in Table I. These markers are useful for studying hydrogen bonding (thymidine H-3), the minor groove (adenosine H-2), the major groove (thymidine CH_3-5), and the sugar–phosphate backbone (adenosine H-8 and thymidine H-6). We observe similar chemical shifts and inter base pair NOEs for these proton markers in the TATA 12-mer (Patel et al., 1983b) and TATA 16-mer duplexes indicative of similar conformations for the TATA box in these two duplexes.

We are unable to definitively assign the partially resolved resonances in the phosphorus spectra of the TATA 12-mer and TATA 16-mer duplexes. The phosphorus assignments of Connolly & Eckstein (1984) for d(GGAATTCC) suggest that the two phosphates at highest field be assigned to the TATA box segment in the center of the TATA 12-mer and TATA 16-mer duplexes.

We have not attempted to assign the protons of the dG·dC base pairs in the TATA 12-mer and TATA 16-mer duplexes. The chemical shifts of the nonterminal dG·dC base pairs are poorly resolved because of the alternating $(dC\text{-}dG)_n$ nature of the sequence and can only be accurately assigned by two-dimensional techniques. We are limited to one-dimensional methods due to sample limitations at this time.

Conformational Transitions. We detect several conformational transitions in addition to the helix–coil transition in our studies of the TATA 12-mer and TATA 16-mer duplexes as a function of nucleic acid and counterion concentration and temperature. The majority of the proton NMR investigations, except where stated otherwise, were undertaken on 333 A_{260}/mL oligonucleotides in 0.1 M phosphate with a factor of 2 dilution for the corresponding phosphorus spectra.

(*A*) *Noncooperative Premelting Transition.* We detect a noncooperative premelting transition for the TATA 12-mer (Figure 5A) and the TATA 16-mer (Figure 5B) that is most pronounced at the dA·dT base pairs in these duplexes. Drew & Dickerson (1981) have observed a spine of hydration in the minor groove of the dA·dT-rich tetranucleotide core in single crystals of the AATT 12-mer duplex. Disruption of the hydration layer with increasing temperature could be reflected in the chemical shift variations associated with changes in propeller twists and minor groove dimensions.

(*B*) *Cooperative Premelting Transition.* A cooperative premelting change is monitored by chemical shift and lineshape changes of the backbone phosphates (Figure 6B) and base proton resonances of the TATA 12-mer duplex between 50 and 60 °C. We observe the thymidine CH_3-5 resonances to shift to low field during this transition, which suggests disruption of the duplex in the TATA box segment of the TATA 12-mer. Similarly, the most pronounced line-width and chemical shift changes are associated with the highest field phosphates (Figure 6B), which have been tentatively assigned to the TATA box segment of the TATA 12-mer duplex. By contrast, neither NMR (Patel et al., 1982b) nor calorimetric (Marky et al., 1983) measurements detect a premelting transition for the AATT 12-mer duplex under the same conditions of high DNA and counterion concentrations.

(*C*) *B to Z Transition.* There is much interest whether the Z helix is formed when one or more dA·dT base pairs replace dG·dC base pairs in the $(dC\text{-}dG)_n$ duplexes. Phosphorus NMR can readily detect this transition since both pyrimidine–purine and purine–pyrmidine phosphates resonate at ~4.2 ppm in B DNA while for Z DNA the chemical shifts are ~3 ppm for the purine–pyrimidine phosphates and ~4.2 ppm for the pyrimidine–purine phosphates (Patel et al., 1979; Eckstein, 1983).

The absence of a 3.0 ppm Z-helix resonance for TATA 12-mer in saturating salt solution (Figure 7A) demonstrates that neither the dG·dC nor the dA·dT base pairs switch to the Z helix. We detect a minor peak in the TATA 16-mer duplex in saturating salt solution (Figure 7B) corresponding to ~11% Z-helix formation. Thus, it is apparent that the central TATA segment in the fully alternating 16-mer inhibits formation of the Z helix in the flanking hexanucleotide $(dC\text{-}dG)_n$ segments.

Hydrogen Exchange Kinetics. We have previously demonstrated a sequence dependence to the hydrogen exchange kinetics in dA·dT base pairs in dodecanucleotide duplexes (Patel et al., 1983b). Specifically, the dA·dT base pairs in the center of the fully alternating TATA 12-mer duplex exchange a factor of 2–3 faster than the corresponding protons at the same positions in the AATT 12-mer duplex. These exchange parameters are a direct measure of the rate constants for transient opening of individual dA·dT base pairs in the dodecanucleotide duplexes and demonstrate faster opening kinetics for the TATA box region compared to the related AATT segment (Patel et al., 1983b). It is important to stress that these data were measured between 30 and 52.5 °C, conditions under which the TATA 12-mer is a fully paired duplex in 0.1 M phosphate.

This paper reports on the hydrogen exchange kinetics of the TATA 16-mer duplex in 0.1 M phosphate at 37.5 °C (Figure 4). We note that the imino protons of dA·dT base pairs 1 and 2 and dG·dC base pairs 3 and 4 exhibit similar kinetics in the TATA 12-mer (Chart Ia) and TATA 16-mer (Chart Ib) duplexes at this temperature (Table II). Thus, the transient helix opening kinetics in the TATA box is independent of the length of the flanking $(dC\text{-}dG)_n$ segments.

Further, the imino protons of dA·dT base pairs 1 and 2 exchange roughly a factor of 3 faster than flanking dG·dC base pairs 3 and 4 in the TATA 12-mer and TATA 16-mer duplexes in 0.1 M phosphate at 37.5 °C (Table II). This explains why the imino protons of the central dA·dT base pairs broaden out at lower temperatures than the flanking dG·dC base pairs for the TATA 12-mer (Figure 3A) and TATA 16-mer (Figure 3B) duplexes in 0.1 M phosphate solution.

The research of Lu and co-workers (1983) and our data (Patel et al., 1983) demonstrate that dA·dT imino protons for specific sequences in the center of the duplex can broaden prior to imino protons of base pairs closer to the ends of the helix. This introduces a word of caution for imino proton assignments in DNA fragments where it has been assumed that broadening occurs in a sequential manner on proceeding from the ends to the interior of the helix.

Loop–Duplex Equilibrium. The TATA 12-mer and TATA 16-mer duplexes adopt a loop conformation at low DNA (33 A_{260}/mL) and low counterion (1 mM sodium phosphate) concentrations. The imino and nonexchangeable protons (Figure 8) and backbone phosphates (Figure 10) can readily differentiate between fully paired duplex and loop conformations.

We locate chain reversal at the TATA segment of the TATA 12-mer on the basis of downfield shifts of the adenosine H-2 protons from 7.2 to 7.3 ppm in the fully paired duplex (Figure 8A) to 8.0–8.1 ppm in the loop conformation (Figure 8B). The downfield shifts of the adenosine H-2 protons reflect loss of ring current contributions from adjacent purines on partner strands on proceeding from a fully-paired duplex to a loop conformation.

The thymidine imino protons in the TATA 12-mer loop conformation resonate at ~11 ppm (Figure 8B) in a spectral region where there are no corresponding protons in the fully paired duplex (Figure 8A). The 10–11 ppm spectral region provides a convenient window for monitoring loop structures and should apply equally well for studies on longer DNA sequences. The thymidine imino protons in the TATA 12-mer loop conformation exhibit exchange rates that are intermediate between the fast values observed for terminal base pairs and the slower values observed for internal base pairs (Figure 9). This suggests that the thymidine imino protons in the TATA 12-mer loop are partially shielded from solvent water as previously observed for hairpin loops that are unable to form fully paired duplexes (Haasnoot et al., 1981, 1983).

The NMR studies on the TATA 12-mer (33 A_{260}/mL) in 1 mM phosphate also demonstrate a salt-dependent equilibrium between a loop conformation in the absence of salt (Figure 8B) and a fully paired duplex in 0.4 M NaCl (Figure 8A). Such a salt-dependent equilibrium has also been detected for the AATT 12-mer duplex at low DNA and counterion concentration (Marky et al., 1983) by optical and circular dichroism measurements. These studies assigned that AATT 12-mer loop conformation to a hairpin helix (Marky et al., 1983) while our NMR studies cannot differentiate between a hairpin helix and a bulge duplex for the TATA 12-mer loop conformation at this time.

The loop conformations of the TATA 12-mer and TATA 16-mer exhibit well-resolved phosphorus resonances to low (3.6 ppm) and to high field (4.6 and 5.0 ppm) (Figure 10A,B) of the 4.0–4.5 ppm spectral dispersion characteristic of the fully paired duplex state. These resonances provide convenient markers of loop formation, and their location in spectral windows indicates that they will remain useful markers for

longer sequences. Similar shifted resonances have been observed in transfer RNA (Gueron & Shulman, 1975), and we assign the shifted resonances in the TATA 12-mer and TATA 16-mer to altered phosphodiester configurations for residues involved in chain reversal to generate the loop structures.

Summary

We summarize below structural and dynamic conclusions based on our proton and phosphorus NMR studies of the fully alternating d(C-G-C-G-T-A-T-A-C-G-C-G) TATA 12-mer and d(C-G-C-G-C-G-T-A-T-A-C-G-C-G-C-G) TATA 16-mer duplexes, which contain a central TATA box flanked by dG·dC base pairs. The exchangeable and nonexchangeable base protons of dA·dT base pairs 1 and 2 in the TATA 12-mer and TATA 16-mer in 0.1 M phosphate have been assigned at high DNA concentrations (333 A_{260}/mL) from one-dimensional NOE measurements at low temperature. These markers monitor a noncooperative premelting transition that is assigned to temperature-dependent variations in the base-pair overlaps most likely resulting from release of tightly bound water lining the minor groove of the TATA box with increasing temperature. The backbone phosphates and nonexchangeable base protons of the TATA box detect another premelting transition, more cooperative in nature, which reflects a conformational transition from a fully paired duplex to a loop structure prior to the onset of the melting transition.

The hydrogen exchange kinetics of the imino protons in the TATA 12-mer (Patel et al., 1983b) and the TATA 16-mer (333 A_{260}/mL) in 0.1 M phosphate can be monitored from line-width and relaxation time measurements in H_2O solution. We demonstrate faster hydrogen exchange rates for the imino protons of dA·dT base pairs in the center of the helix compared to those of the flanking dG·dC base pairs at the duplex level. We also observe a sequence dependence to hydrogen exchange, which in turn is a measure of transient duplex opening rates with much faster kinetics for the imino protons of the dA·dT base pairs in the TATA box compared to the corresponding AATT segment.

We are interested in the sequence- and base-dependence requirements of the B to Z transition in fully alternating pyrimidine–purine oligonucleotides in high-salt solution. We demonstrate that the incorporation of the four base pair TATA segment totally inhibits the B to Z transition of the flanking $(dC\text{-}dG)_2$ segments in the TATA 12-mer in saturating salt solution. By contrast, we detect the onset of the B to Z transition in the TATA 16-mer in saturating salt due to the longer length of the flanking $(dC\text{-}dG)_3$ segments.

The proton and phosphorus NMR parameters monitor a conformational equilibrium between the fully paired duplex and a loop conformation for the TATA 12-mer and the TATA 16-mer with the loop structure favored at low DNA (33 A_{260}/mL), low counterion (1 mM phosphate), and elevated temperatures. The loop conformation can be readily detected by monitoring the imino protons (10–11 ppm) and backbone phosphates (3.5–4.0 ppm; 4.5–5.0 ppm) involved in chain reversal as they fall in spectral windows devoid of other resonances. We are unable to differentiate between a hairpin helix and a bulge duplex for the loop conformation of the TATA 12-mer and TATA 16-mer at this time.

Acknowledgments

The high-field NMR experiments were performed at the NMR facility for Biomedical Research at the Francis Bitter National Magnet Laboratory, Massachusetts Institute of Technology. The NMR facility is supported by Grant RR0095 from the Division of Research Resources of the National Institutes of Health and by the National Science Foundation under Contract C-670. The 500-MHz NMR spectra at low DNA concentrations were recorded at the University of Washington, Seattle, and the facility was funded by the Murdock Foundation and National Institutes of Health Grant 3R01-GM28764-01S1. The DNA synthesis portion of the research was funded by National Institutes of Health Grant GM31259 to K.I.

Registry No. TATA 12-mer, 85684-25-9; TATA 16-mer, 94293-94-4.

References

Arnott, S. Chandrasekaran, R., Banerjee, A. K., He, R., & Walker, J. K. (1983) *J. Biomol. Struct. Dyn. 1*, 437–452.
Calladine, C. R. (1982) *J. Mol. Biol. 161*, 343–362.
Calladine, C. R., & Drew, H. R. (1984) *J. Mol. Biol. 178*, 773–782.
Clore, G. M., & Gronenborn, A. M. (1983) *EMBO J. 2*, 2109–2115.
Connolly, B. A., & Eckstein, F. (1984) *Biochemistry 23*, 5523–5527.
Dickerson, R. E. (1983) *J. Mol. Biol. 166*, 419–441.
Dickerson, R. E., & Drew, H. R. (1981) *J. Mol. Biol. 149*, 761–768.
Dickerson, R. E., Drew, H. R., Conner, B. N., Wing, R. M., Fratini, A. V., & Kopka, M. L. (1982) *Science (Washington, D.C.) 216*, 475–485.
Dickerson, R. E., Kopka, M. L., & Drew, H. R. (1983) in *Structure and Dynamics: Nucleic Acids and Proteins* (Clementi, E., & Sarma, R. H., Eds.) pp 149–479, Adenine Press, New York.
Drew, H. R., & Dickerson, R. E. (1981) *J. Mol. Biol. 151*, 535–556.
Early, T. A., Kearns, D. R., Hillen, W., & Wells, R. D. (1981a) *Biochemistry 20*, 3756–3764.
Early, T. A., Kearns, D. R., Hillen, W., & Wells, R. D. (1981b) *Biochemistry 20*, 3764–3769.
Eckstein, F. (1983) *Angew. Chem., Int. Ed. Engl. 22*, 423–439.
Feigon, J., Wright, J. M. Denny, W. A., Leupin, W., & Kearns, D. R. (1983) *Cold Spring Harbor Symp. Quant. Biol. 47*, 207–217.
Fritzche, H., Kan, L. S., & Ts'o, P. O. P. (1983) *Biochemistry 22*, 277–280.
Giessner-Prettre, C., Pullman, B. Borer, P. N., Kan, L. S., & Ts'o, P. O. P. (1976) *Biopolymers 15*, 2277–2286.
Gorenstein, D. G., & Luxon, B. A. (1979) *Biochemistry 18*, 3796–3804.
Gorenstein, D. G., Findlay, J. B., Momii, R. K., Luxon, B. A., & Kar, D. (1976) *Biochemistry 15*, 3796–3803.
Gueron, M., & Shulman, R. G. (1975) *Proc. Natl. Acad. Sci. U.S.A. 72*, 3482–3485.
Haasnoot, C. A., de Bruin, S. H., Berendsen, R. G. Janssen, H. G., Binnendijk, T. J., Hilbers, C. W., van der Marel, G. A., & van Boom, J. H. (1983) *J. Biomol. Struct. Dyn. 1*, 115–129.
Haasnoot, C. A. G., den Hartog, J. H., de Rooij, J. F., van Boom, J. H., & Altona, C. (1980) *Nucleic Acids Res. 8*, 169–181.
Haniford, D. B., & Pulleyblank, D. E. (1983) *Nature (London) 302*, 632–634.
Hare, D. R. Wemmer, D. E., Chou, S. H., Drobny, G., & Reid, B. R. (1983) *J. Mol. Biol. 171*, 319–336.
Joseph, A. P., & Bolton, P. H. (1984) *J. Am. Chem. Soc. 16*, 437–439.

Jovin, T. M., McIntosh, L. P., Arndt-Jovin, D. J., Zarling, D. A., Robert-Nicoud, M., van de Sande, J. H., Jørgensen, K. F., & Eckstein, F. (1983a) *J. Biomol. Struct. Dyn. 1*, 21–55.

Jovin, T. M., van de Sande, J. H., Zarling, D. A., Arndt-Jovin, D. J., Eckstein, F., Fuldner, H. H., Greider, C., Greiger, I., Hamori, E., Kalisch, B., McIntosh, L. P., & Robert-Nicoud, M. (1983b) *Cold Spring Harbor Symp. Quant. Biol. 47*, 143–154.

Klysik, J., Stirdivant, S. M., Larson, J. E., Hart, P. A., & Wells, R. D. (1981) *Nature (London) 290*, 672–677.

Lu, P., Cheung, S., & Arndt, K. (1983) *J. Biomol. Struct. Dyn. 1*, 509–521.

Marky, L., Blumenfeld, K. S., Kozlowski, S., & Breslauer, K. (1983) *Biopolymers 22*, 1247–1257.

Marky, N. L., & Olson, W. K. (1982) *Biopolymers 21*, 2329–2344.

Mirau, P. A., & Kearns, D. R. (1983) *Structure and Dynamics: Nucleic Acids and Proteins* (Clementi, E., & Sarma, R. H., Eds.) pp 227–239, Adenine, New York.

Nordheim, A., & Rich A. (1983) *Nature (London) 303*, 674–679.

Pardi, A., & Tinoco, I. (1982) *Biochemistry 21*, 4686–4693.

Pardi, A., Martin, F. H., & Tinoco, I. (1981) *J. Am. Chem. Soc. 20*, 3980–3996.

Patel, D. J. (1976) *Biopolymers 15*, 533–558.

Patel, D. J., & Hilbers, C. W. (1975) *Biochemistry 14*, 2651–2656.

Patel, D. J., Canuel, L. L., & Pohl, F. M. (1979) *Proc. Natl. Acad. Sci. U.S.A. 76*, 2508–2511.

Patel, D. J., Pardi, A., & Itakura, K. (1982a) *Science (Washington, D.C.) 216*, 581–590.

Patel, D. J., Kozlowski, S. A., Markly, L. A., Broka, C., Rice, J. A., Itakura, K., & Breslauer, K. J. (1982b) *Biochemistry 21*, 428–436.

Patel, D. J., Kozlowski, S. A., Nordheim, A., & Rich, A. (1982c) *Proc. Natl. Acad. Sci. U.S.A. 79*, 1413–1417.

Patel, D. J., Kozlowski, S. A., & Bhatt, R. (1983a) *Proc. Natl. Acad. Sci. U.S.A. 80*, 3908–3912.

Patel, D. J., Ikuta, S., Kozlowski, S. A., & Itakura, K. (1983b) *Proc. Natl. Acad. Sci. U.S.A. 80*, 2184–2188.

Petersheim, M., Mehdi, S., & Gerlt, J. A. (1984) *J. Am. Chem. Soc. 106*, 439–440.

Pohl, F. M., & Jovin, T. M. (1982) *J. Mol. Biol. 67*, 375–396.

Redfield, A. G., Roy, S., Sanchez, V., Tropp, J., & Figueroa, N. (1981) in *Biomolecular Stereodynamics* (Sarma, R., Ed.) pp 195–208, Adenine, New York.

Rich, A., Nordheim, A., & Azorin, F. (1983) *J. Biomol. Struct. Dyn. 1*, 1–19.

Rich, A., Nordheim, A., & Wang, A. (1984) *Annu. Rev. Biochem. 53*, 791–846.

Salemink, P. J., Reijerse, E. J., Molevanger, L. C., & Hilbers, C. W. (1981) *Eur. J. Biochem. 115*, 635–641.

Scheffler, I. E., Elson, E. L., & Baldwin, R. L. (1968) *J. Mol. Biol. 36*, 291–304.

Shakked, Z., Rabinowich, D., Cruse, W. B., Egert, E., Kennard, O., Sala, G., Salisbury, S. A., & Viswamitra, M. A. (1981) *Proc. R. Soc. London, Ser. B 213*, 479–487.

Singleton, C. K., Klysik, J., Stirdivant, S. M., & Wells, R. D. (1982) *Nature (London) 299*, 312–316.

Tan, Z. K. Ikuta, S., Haung, T., Dugaiczyk, A., & Itakura, K. (1983) *Cold Spring Harbor Symp. Quant. Biol. 47*, 383–391.

Wang, A. H., Quigley, G. J., Kolpak, F. J., Crawford, J. L., van Boom, J. H., van der Marel, G., & Rich, A. (1979) *Nature (London) 282*, 680–686.

Wang, A. H. Fujii, S., van Boom, J. H., & Rich, A. (1982) *Proc. Natl. Acad. Sci. U.S.A. 79*, 3968–3972.

Weiss, M., Patel, D. J., Sauer, R. T., & Karplus, M. (1984) *Proc. Natl. Acad. Sci. U.S.A. 81*, 130–134.